16TH EUROPEAN CONFERENCE ON EARTHQUAKE ENGINEERING THESSALONIKI 18 - 21 JUNE 2018

MOTIVES FOR A MULTIDIRECTIONAL CONDITIONAL SPECTRUM IN SEISMIC DESIGN AND ASSESSMENT

Cecilia I. NIEVAS[1], Timothy J. SULLIVAN[2]

ABSTRACT

While the seismic design of structures has traditionally been carried out considering two perpendicular horizontal components of ground shaking, real ground motions are complex and can impose very different demands at different orientations of the building with respect to the seismic source. The relevance of this complexity and its influence on the seismic performance of different kinds of structures has, thus, been receiving increasing attention in recent years. The authors of this paper have recently focused their research efforts in studying ways to provide an encompassing definition of seismic demands that aims at designing engineering structures whose relative performance does not depend on their sensitivity to the angle of incidence of ground motion. The multidirectional conditional spectrum resulted from this framework and has been recently proposed by the authors as a tool to characterise seismic demands at different angles of incidence. This paper focuses on explaining the motives and need for such a tool, and describes in detail the three main components needed for its generation. Examples are given and the relevance of accounting for the correlation between demands at different angles is illustrated. Applications and future developments are finally discussed.

Keywords: bi-directional excitation; directionality; conditional spectrum; record selection; rotationally-dependent demands

1. INTRODUCTION

The relevance of accounting for the variation of seismic demands at different orientations has been receiving increasing attention in recent years. The notion that as-recorded components of ground motion need not necessarily represent the largest or median demands has prompted the inspection of ways to incorporate the uncertainty in the angle of incidence and its consequent influence on demands to the design and assessment of structures (Boore et al. 2006; Hong and Goda 2007; Boore 2010). Almost concurrently, acknowledgment that the uniform hazard spectrum combines values with equal probability of individual occurrence, but a much lower probability of occurring simultaneously, led to the development of the Conditional Spectrum (CS, Baker and Cornell 2006), which has become a popular tool to characterise the expected seismic demands at different oscillator periods and their associated variability, conditioned on the occurrence of a particular demand at a particular period that serves as an anchor. The CS is a powerful tool that can be combined with recent developments in the characterisation of the variation of ground motions at different angles of incidence to generate a set of conditional spectra at different directions that is anchored not only to a specific maximum rotationally-dependent pseudo-spectral acceleration at a certain period, $Sa_{RotD100}(T^*)$, but also to the direction at which it occurs.

Recognising the points above, Nievas and Sullivan (2017) have developed a Multidirectional Conditional Spectrum (MDCS), which is, in fact, a series of pseudo-acceleration response spectra at different orientations with respect to the direction of maximum response at the anchoring period. The

[1]ROSE Programme, UME School, IUSS Pavia, Italy, nievas.cecilia.i@gmail.com
[2]Department of Civil and Natural Resources Engineering, University of Canterbury, Christchurch, New Zealand, timothy.sullivan@canterbury.ac.nz

spectra are defined both in terms of expected values and their associated dispersions. The present paper discusses in detail the motives for such an endeavour, and goes through the main components that need to be combined for their generation, as well as the associated numerical procedure. The characteristics of the resulting spectra are presented, and their possible applications and associated future developments are discussed.

2. THE NEED FOR MULTIDIRECTIONAL CONDITIONAL SPECTRA

The seismic design of structures is usually carried out considering horizontal ground motions occurring in perpendicular directions that often coincide with the main axes of the building plan. At the same time, accelerometers record ground motions along three mutually perpendicular axes. During many decades, only acceleration values recorded along these axes, or an arithmetic or geometric mean of the two, were taken into consideration for the characterization of seismic hazard. After many years, it was finally acknowledged that none of these measures necessarily represented what was happening at other orientations, and that those of the recording instrument could be related in any way to those of the structures being designed and, in general, to faults themselves. This realisation gave birth to rotational definitions of horizontal ground motion such as the X^{th} percentile rotationally-dependent and independent components or geometric means (i.e. $RotD_X$, $RotI_X$, $GMRotD_X$, $GMRotI_X$; Boore et al. 2006; Boore 2010).

While these definitions of intensity help overcome the issue of ground motion dependence on the orientation of the recording devices, they provide no specific information regarding what happens at all possible orientations. Great advances in this respect have been made by Hong and Goda (2007) and Shahi and Baker (2014). The former studied the behaviour of the ratio of the spectral acceleration at an angle θ from the direction of maximum response, that is, the direction at which $Sa_{RotD100}(T)$ occurs, and $Sa_{RotD100}(T)$ itself, which they called η(T,θ). Hong and Goda (2007) found that when representing η(T,θ) in a polar plot whose horizontal axis is the direction of maximum response, η(T,θ) always falls outside two small circles with a radius of 0.5, each of them centred at (-0.5,0.0) and (0.5,0.0), and they named this the *goggle phenomenon* (Figure 1). This implies that, at any angle θ, η(T,θ) is bounded by [|cos θ|,1.0], and that the statistical behaviour of η(T,θ) can be represented by a generalised Beta distribution. The most important derivation of the work of Hong and Goda (2007) is that the probability of exceeding a certain value of spectral acceleration at a certain angle can be split into two separate problems, one associated to $Sa_{RotD100}(T)$ and the other associated to η(T,θ).

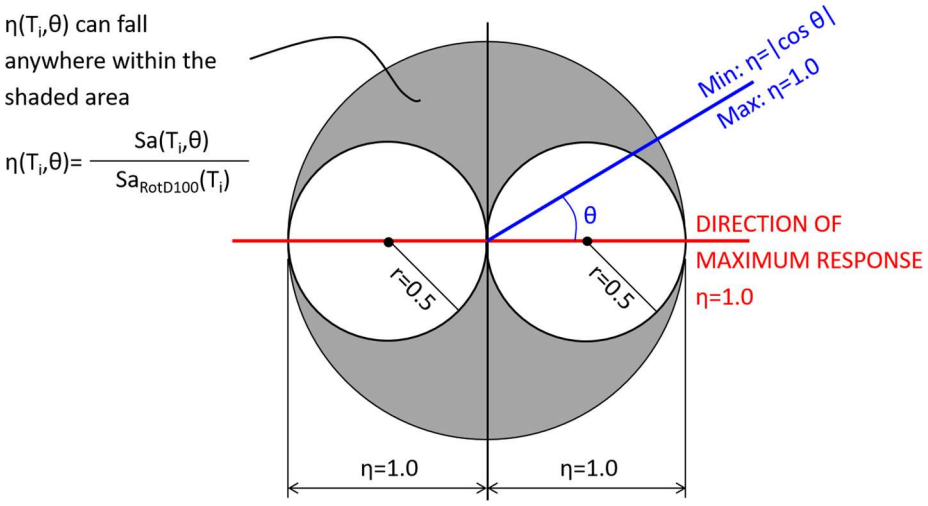

Figure 1. Schematic representation of the ratio η(T,θ) (ratio of Sa(T,θ) to $Sa_{RotD100}(T)$) and the goggle phenomenon described by Hong and Goda (2007).

More recently, Shahi and Baker (2014) have developed a series of models to characterise a series of parameters related to direction-dependent spectra. Having worked within the NGA-West2 research programme (Bozorgnia et al. 2014), they studied in detail the behaviour of the ratio of $Sa_{RotD100}(T)$ to $Sa_{RotD50}(T)$, the latter being the metric used by the NGA-West2 ground motion prediction models, as well as the orientation of $Sa_{RotD100}(T)$ with respect to the strike-normal and strike-parallel directions, and the relation between the orientations of $Sa_{RotD100}(T)$ at different oscillator periods. Based on this, Shahi and Baker (2014) also outlined an initial framework for the generation of orientation-specific spectra, using $Sa_{RotD50}(T)$ as a starting point.

From the engineering perspective, efforts on the subject of directionality have been divided in two main areas. On the one hand, a large number of studies have been conducted to assess the influence of applying sets of ground motions to three-dimensional models of structures at different angles of incidence (e.g. Lagaros 2010; Magliulo et al. 2014; Kalkan and Reyes 2015). On the other, only a few appear to have focused on trying to bridge the gap between seismology and engineering, and taking advantage of the recent advances in the former to define ground motion demands at different orientations at the stage in which the seismic hazard assessment is carried out, instead of aiming to solve the question of directionality at the very last stage of structural design. Within these, the work of Grant (2011) and Stewart et al. (2011) are of special significance, because they highlight the need to take into consideration the characteristics of different structural typologies when defining appropriate seismic loads for their design. As they point out, structures can be broadly classified into two kinds: those which, as a consequence of their axial symmetry in strength and stiffness, are always subject to the largest horizontal component of ground motion (e.g. a circular tank), and those for which the angle of incidence of ground motion can exert a large influence on the demands they are subject to. Imagining two structures with the same fundamental period, one of each kind, designed for the same spectral demand and subject to a ground motion with said spectral demand, the former, the so-called *azimuth-independent* structure, would always be subject to its design demand, while the latter, the *azimuth-dependent* structure, could be subject to much less, depending only on the relative orientation of the building with respect to the seismic source.

The summation of all these contributions led Nievas (2016) to study ways to provide an encompassing definition of seismic demands aimed at guaranteeing that the seismic performance of a building does not depend on its sensitivity to the angle of incidence of ground motion. As a first step, Nievas and Sullivan (2016) addressed the concerns of Grant (2011) and Stewart et al. (2011) and showed how the findings of Hong and Goda (2007) can be used to define seismic demands for different structural typologies. As that initial work focused primarily on single-degree-of-freedom systems, the fact that most structures are multi-degree-of-freedom instead prompted the interest in the development of spectra that could gather state-of-the-art knowledge regarding demands at different orientations in a way that could be useful for design and assessment. The main components were already available: conditional spectra, a certain degree of understanding of the behaviour of the $\eta(T,\theta)$ ratio, and a model to characterise the relation between orientations of demands at different periods. Complementary components and models were assessed and developed, as described in Nievas and Sullivan (2017).

As a consequence of the broader research effort within which work on the multidirectional conditional spectrum was framed, $Sa_{RotD100}(T)$ was preferred as a starting point because of its relevance for azimuth-independent structures (thinking within a scheme appropriate for all typologies), and because the behaviour of the $\eta(T,\theta)$ ratio, with its natural $[|\cos\theta|,1.0]$ bounds, appears as much more intuitive than that of $Sa_{RotD100}(T)/Sa_{RotD50}(T)$ (used by Shahi and Baker 2014) to introduce the concept of directionality to the design office.

The following sections describe the components and procedure needed to generate multidirectional conditional spectra, and provide examples of their outcome. While details on the numerical procedure and each of the models and equations used are provided in Nievas and Sullivan (2017), focus is herein placed on explaining the way in which all the pieces fit together.

3. GENERATION OF MULTIDIRECTIONAL CONDITIONAL SPECTRA

As explained in Nievas and Sullivan (2017), three main components are needed for the generation of MDCS:

1. Characterisation of the ground motion demands by means of a CS in terms of the maximum response component, $Sa_{RotD100}(T)$.
2. Characterisation of the relation between the orientations of the maximum response directions at different oscillator periods.
3. Characterisation of the variation of the spectral acceleration at different angles and its relation with the maximum response component, $Sa_{RotD100}(T)$.

The relation between the three is illustrated in Figure 2. The CS in terms of $Sa_{RotD100}(T)$, generated for a certain anchoring period T* with a pre-defined spectral acceleration demand Sa_{RD100}*, describes the values of $Sa_{RotD100}(T)$ that are reasonably expected to occur together with Sa_{RD100}*, taking into consideration the correlation between spectral demands at different oscillator periods, for which an appropriate model is needed. At any period T_i there is an expected (mean) value, and an associated standard deviation. As shown in Figure 2, a log-normal distribution is assumed (Jayaram and Baker, 2008). Though the distribution is continuous, one can imagine it as a succession of finite possible values of $Sa_{RotD100}(T_i)$, each with an associated probability of occurring.

Each of these values $Sa_{RotD100}(T_i)_j$ can occur at a certain angle α with respect to the direction at which Sa_{RD100}* occurs. Shahi and Baker (2014) observed that the likelihood of α to be small, that is, of the two directions of maximum response to be aligned, is larger if the periods are closely spaced than if they are more distant from each other, and developed a model that allows to calculate this likelihood for any two periods and any angle α. The existence of this angle α and the definition of the maximum response component $Sa_{RotD100}(T)$ imply that, for each value *j* of $Sa_{RotD100}(T_i)_j$, Sa_{RD100}* occurs simultaneously with a spectral acceleration value at T_i that can be equal to or smaller than $Sa_{RotD100}(T_i)_j$, but never larger. As shown by Hong and Goda (2007), the ratio of the spectral acceleration value at an angle α with respect to $Sa_{RotD100}(T_i)_j$ to $Sa_{RotD100}(T_i)_j$ itself can be characterised by a Beta distribution with lower bound equal to |cos α| and upper bound equal to 1.0. Figure 2 shows, as an example, probability densities of this ratio, η(T,θ), for 30º and 90º. At 90º, the lower bound is equal to zero, while at 30º it is equal to 0.866 (θ used instead of α for the reasons that follow).

Simultaneously considering the probability of a particular value of $Sa_{RotD100}(T_i)_j$ occurring, together with the probability of it forming a particular angle α with respect to the direction at which Sa_{RD100}* occurs, together with the probability of a particular value of η occurring at that angle as well allows to calculate the overall probability of $\eta(T_i,\theta)\cdot Sa_{RotD100}(T_i)_j$ occurring at the direction at which Sa_{RD100}* occurs. Considering all possible values of the variables involved and combining them through the total probability theorem allows to calculate a mean expected value for the spectral value at T_i, and a distance between each particular value considered and this mean, which allows in the end to calculate its associated standard deviation.

This whole process can then be repeated at an angle θ_{GL} from the direction at which Sa_{RD100}* occurs. All the considerations made before are then transformed to what happens at an angle $|\theta_{GL} - \alpha|$ instead of simply α (at the direction at which Sa_{RD100}* occurs, $\theta_{GL} = 0º$ and, thus, $|\theta_{GL} - \alpha| = \alpha$). Calling θ_L (*L* for *local*) the absolute difference between the global angle θ_{GL} and α, and assuming a log-normal distribution, the mean and standard deviation of the conditional spectral acceleration at a period Ti and global angle θ_{GL} can be calculated as per Equations 1 and 2 below:

$$\overline{\ln Sa(T_i,\theta_{GL})} = \sum_{j=1}^{40}\sum_{m=0}^{180}\sum_{k=1}^{40}\left\{P\left[Sa_{RotD100,j}(T_i)\right]\cdot P[\alpha_m(T_i,T^*)]\cdot P[\eta_k(T_i,\theta_L)]\cdot \ln\left(Sa_{RotD100,j}(T_i)\cdot\eta_k(T_i,\theta_L)\right)\right\} \quad (1)$$

$$\sigma^2_{\ln Sa(T_i,\theta_{GL})} = \sum_{j=1}^{40}\sum_{m=0}^{180}\sum_{k=1}^{40}\Big\{P\big[Sa_{RotD100,j}(T_i)\big]\cdot P[\alpha_m(T_i,T^*)]\cdot P[\eta_k(T_i,\theta_L)]\cdot \Big[\ln\big(Sa_{RotD100,j}(T_i)\cdot\eta_k(T_i,\theta_L)\big)-\overline{\ln Sa(T_i,\theta_{GL})}\Big]^2\Big\} \quad (2)$$

While a handy closed-form analytical equation to calculate MDCS would be ideal, the variety of distributions associated to each of the parameters involved and the way in which they are all related with each other makes it, at least, challenging. For this reason, Equations 1 and 2 are used herein to generate MDCS by means of a numerical procedure that involves discretising the distributions of each of the main relevant parameters, combining them, and quantifying the final probability of each combination, which is used to weigh the combination to produce the final result (Nievas and Sullivan 2017).

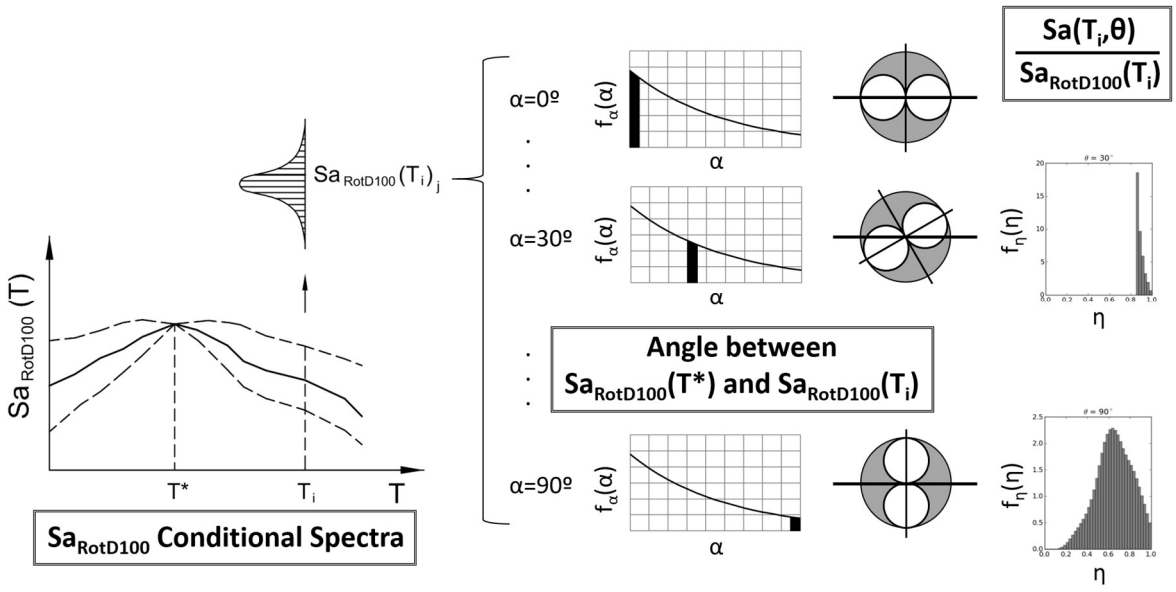

Figure 2. Schematic representation of the three components of multidirectional conditional spectra

While Equations 1 and 2 assume that it is appropriate to work in the logarithmic space, the fit between results obtained by Nievas and Sullivan (2017) and the log-normal distribution is not perfect, as MDCS result from the combination of log-normal (the CS), generalised Beta (for η(T,θ)) and truncated exponential (for α) distributions. Non-logarithmic means and standard deviations can be calculated by means of Equations 1 and 2, without taking the natural logarithm of the data.

The capacity of normal and log-normal distributions to represent the MDCS was assessed by calculating the maximum (absolute) discrepancy between the empirical distribution function (EDF) and the cumulative distribution function (CDF) of the theoretical distributions, as is done for the Lilliefors test of goodness-of-fit. The discrepancy was calculated at each global angle and each oscillator period, and the median across all angles was then calculated for each period. As the size of the sample is undefined, these discrepancies could not be compared against pre-defined thresholds and were compared with each other instead (i.e. those for the normal distribution against those for the log-normal one). Figure 3 shows the difference between the two, with darker colours corresponding to more negative differences, which indicate that a log-normal distribution fits the data better than a normal one, for twelve cases of MDCS (corresponding to different anchoring periods and values of Sa_{RD100}*, along the vertical axis) and 25 oscillator periods (along the horizontal axis). As can be observed, there is a tendency for the log-normal distribution to fit the data better, particularly at periods distant from the anchoring period T*. At T* itself, it is a Beta distribution (hence the cells corresponding to T* being crossed out in the plot of Figure 3), and for this reason there is a transition period range in between the two. While it is noted that it is likely that the MDCS is neither normally

nor log-normally distributed, this assessment is relevant both to understand whether means and standard deviations should be calculated in a linear or a logarithmic space, and to open the door to possible simplifications in the generation of MDCS in the future. It should be always borne in mind, however, that Sa(T,θ) cannot take on negative values and, in this sense, the log-normal distribution will always be more appropriate than the normal one.

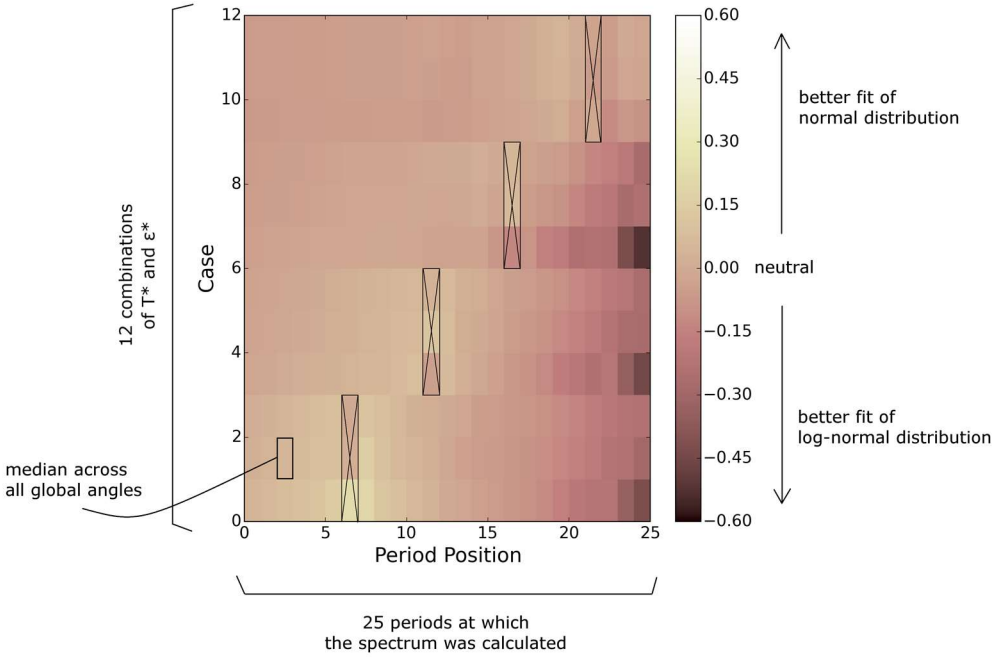

Figure 3. Difference between the median (across all orientations) discrepancy for the log-normal assumption and that of the normal assumption. Discrepancy measured as maximum absolute difference between the EDF and the CDF of the theoretical distributions. Negative values indicate a better fit of the log-normal distribution.

4. EXAMPLE

Figure 4 shows an example of MDCS calculated for T*=1.0 s, Sa_{RD100}*=0.1 g, mean causal earthquake magnitude, distance and V_{s30} of 5.5, 20 km and 760 m/s, respectively. The CS was constructed using the ground motion prediction equation of Hong and Goda (2007), as implemented in OpenQuake (Pagani et al. 2014), and the correlation model adjusted by Nievas and Sullivan (2017). The probability of each angle α between the directions of maximum response at different periods was calculated with the model of Shahi & Baker (2014). The variation of demand at all possible orientations, characterised by the ratio $\eta(T_i,\theta)$ of $Sa(T_i,\theta)$ at an arbitrary angle and $Sa_{RotD100}(T_i)$, was modelled by means of the kernel density estimations derived by Nievas and Sullivan (2017) using data from the RESORCE database (Akkar et al. 2014). As is apparent in the plots, MDCS are not just a set of expected values but, most importantly, a complete distribution.

As can be observed in Figure 4, spectral demands tend to decrease for increasing angles. At each particular period, they are a minimum at 90º, as shown in Figure 5 (left), and the difference between 0º and 90º is more accentuated at T* than at the rest of the periods. This is due to the tendency of the directions of maximum response at periods that are sufficiently close to each other to be relatively aligned, which is quickly lost when the periods grow further apart. At T* itself, no value other than Sa_{RD100}* can occur at θ_{GL}=0º. At more distant periods, the probability of the angle α being any value becomes more uniform as per the model of Shahi and Baker (2014), causing spectral demands to be more averaged out at any possible orientation. This is reflected in the standard deviation, which also presents its largest variation at T* itself (Figure 5, right): it is zero at θ_{GL}=0º and has its maximum at θ_{GL}=90º. As shown in Figure 5, MDCS are symmetric with respect to 90º (e.g., the spectrum at θ_{GL}=70º is the same as that θ_{GL}=110º, and that at θ_{GL}=30º is the same as that at θ_{GL}=150º).

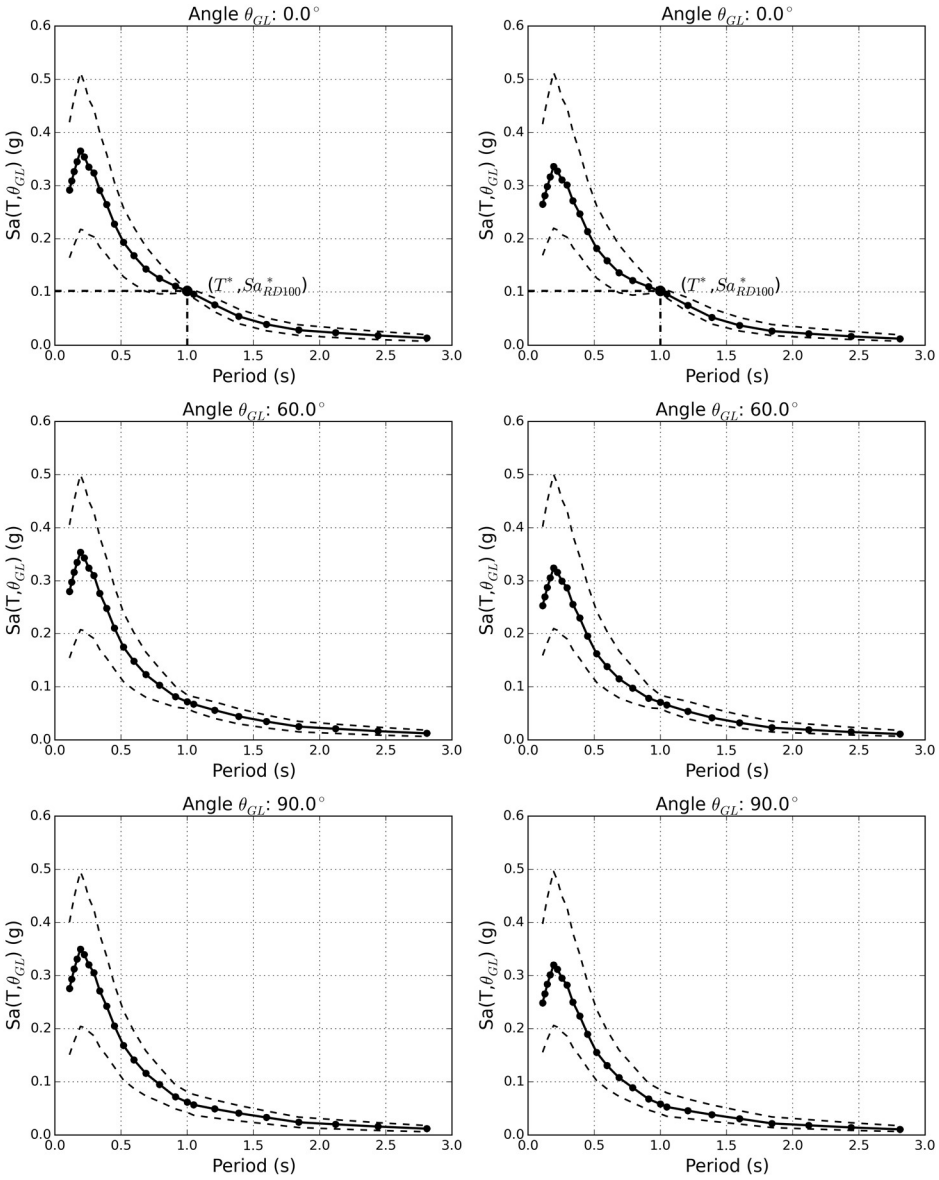

Figure 4. Multidirectional conditional spectra (mean ± one standard deviation) for three different global orientations. T*=1.0 s, Sa_{RD100}*=0.10 g, ε*=1.469. Means and standard deviations calculated in linear (left) and logarithmic (right) spaces.

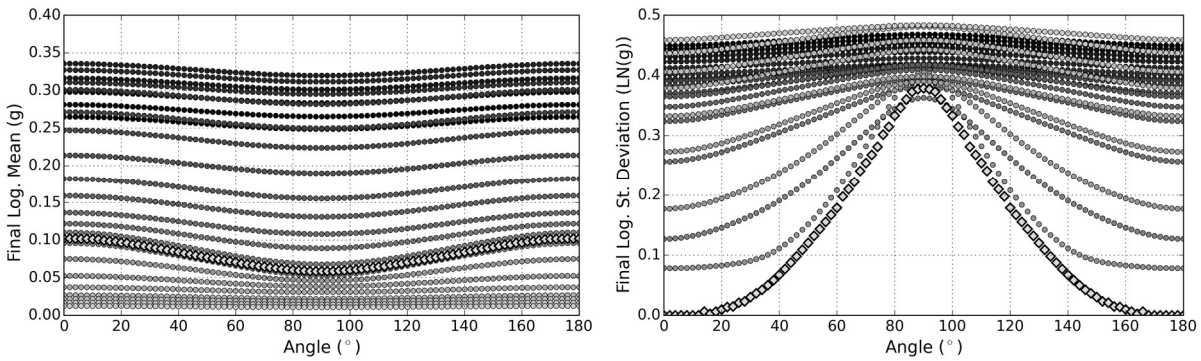

Figure 5. Mean values (left) and standard deviations (right) of Sa(T, θ_{GL}) at each angle θ_{GL} in logarithmic space, for T*=1.0 s, Sa_{RD100}*=0.10 g, and ε*=1.469. Different shades for different periods: darker grey for smaller periods, lighter grey for larger ones. Rhombuses correspond to T*.

5. EFFECTS OF CORRELATION BETWEEN DEMANDS AT DIFFERENT ANGLES

Due to the complexities associated to incorporating the effects of correlation when a large number of different marginal distributions are involved, the procedure described above and the examples shown in Figures 3 and 4 do not consider the correlation between values of $\eta(T_i,\theta)$ for the same period but different angles. As Nievas and Sullivan (2017) show, this correlation can be incorporated by means of Monte Carlos simulations. The plots in Figure 6 compare the results obtained by means of the numerical procedure described above (black lines) and two Monte Carlo Simulations. Results shown in red and labelled *M.Carlo 2* do not incorporate said correlation and serve as a means of verifying that the results from the Monte Carlos simulations can be compared against the numerical procedure (labelled *Analytical* not in contraposition to its numerical nature but to indicate that it stems from an analytical method and not a simulation). Results shown in blue and labelled *M.Carlo 1* do incorporate said correlation, and show that its effect is that of increasing the means and decreasing their associated standard deviation, a tendency that is accentuated the most at θ_{GL}=90º. This suggests that taking correlation into consideration is relevant for the final outcome. Details regarding the incorporation of correlation and the model used can be found in Nievas and Sullivan (2017).

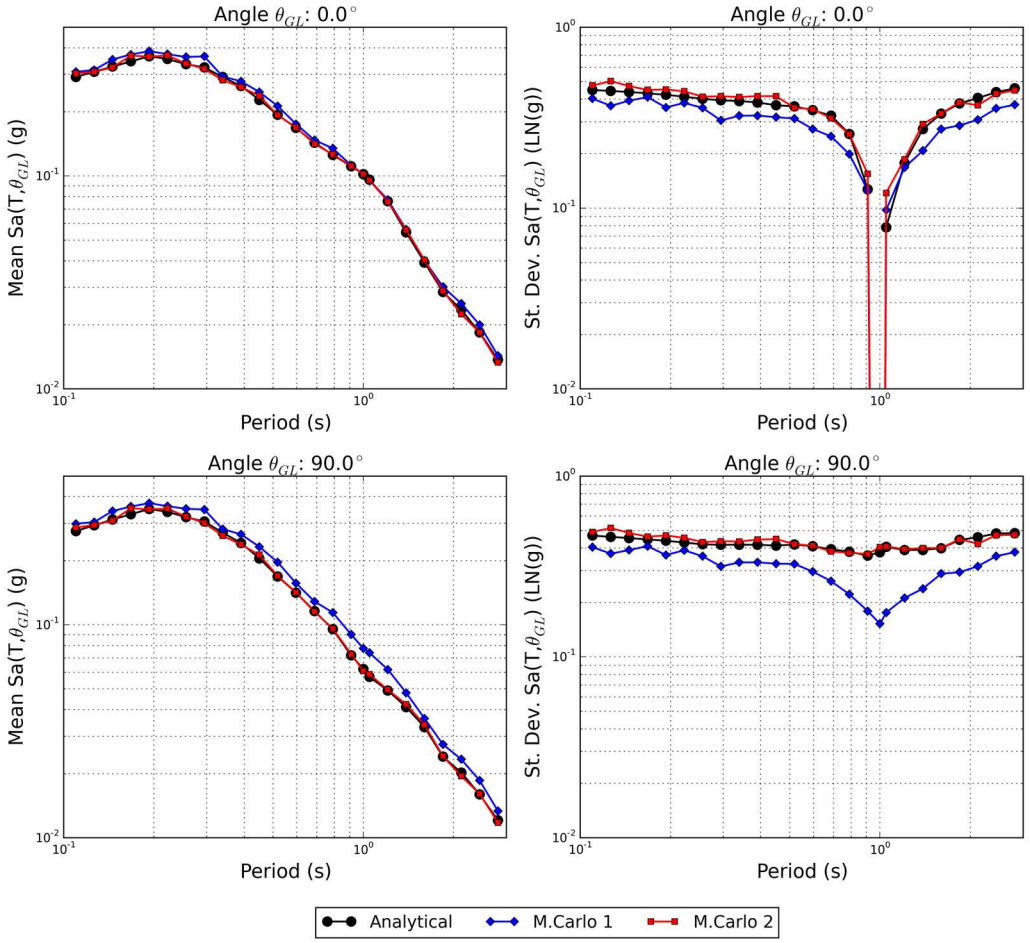

Figure 6. (Logarithmic) means (left) and standard deviations (right) of $Sa(T,\theta_{GL})$ for T*=1.0 s, Sa_{RD100}*=0.10 g, and ε*=1.469, calculated through the numerical procedure (Analytical) and Monte Carlo simulations with (M.Carlo 1) and without (M.Carlo 2) accounting for the correlation between values of $\eta(Ti,\theta)$ for the same period but different angles.

6. APPLICATIONS AND FUTURE DEVELOPMENTS

As MDCS allow for the characterisation of seismic demands at all possible orientations both in terms of their expected values and their standard deviations, they can become a powerful tool for the seismic design and assessment of buildings. The most important question that follows is which orientation of the MDCS to apply along which direction of the structure, together with that of how to combine demands associated to different periods of vibration and directions. The latter has traditionally been addressed by means of modal combination procedures such as the complete quadratic combination (CQC) rule (Der Kiureghian 1981; Wilson et al. 1981), and spatial combination methods such as the 30% rule (Rosenblueth and Contreras 1977) or the complete quadratic combination with three components (CQC3) rule (Smeby and Der Kiureghian 1985; Menun and Der Kiureghian 1998), developed around the 1970s and 1980s. As Nievas (2016) and Nievas and Sullivan (2018) point out, these rules do not account for the large dispersion associated to the problem, and their revision within the context of performance-based engineering appears as timely. Regarding the orientations of demand to consider for design, it is noted that application of the direction of $Sa_{RotD100}(T)$ along the main axes of an azimuth-dependent building would lead to the over conservatism that has already been pointed out by Grant (2011), Stewart et al. (2011) and Nievas and Sullivan (2016), and should consequently be avoided, as it would contradict the spirit with which the MDCS was developed. Future research should, thus, focus on this kind of structure and aim either to develop a correction factor to be applied to the demands at 0º, or to define which two perpendicular directions other than 0º and 90º can be applied to obtain a consistent result. The final goal should be all structural typologies presenting the same probability of exceeding the relevant pre-defined limit states.

As a natural evolution of the conditional spectrum (Baker, 2011), MDCS can also be used for the selection of ground motion records for dynamic structural analyses. Nievas and Sullivan (2017) discuss ways in which the algorithm of Jayaram et al. (2011) can be adapted to be used with MDCS, both assuming that hazard is defined in terms of the maximum response component, $Sa_{RotD100}(T)$, and acknowledging that, at present, it is not. Along these lines, it should be highlighted that the logic behind the MDCS adheres to the embracing of performance-based design and assessment principles by seismic codes, and requires that hazard at a site start being defined in terms of $Sa_{RotD100}(T)$ and $\eta(T,\theta)$. While it is possible to use kernel density estimations like those derived by Nievas and Sullivan (2017), MDCS would certainly benefit from the development of a parametric model to describe the distribution of $\eta(T,\theta)$ at all angles.

7. CONCLUSIONS

This paper has presented the motives and need for a multidirectional conditional spectrum that represents demands at all possible orientations with respect to the direction of maximum response at a conditioning period of interest and the spectral demand associated with it. The three main components needed for its generation, namely, a conditional spectrum in terms of $Sa_{RotD100}(T)$, a model to describe the (lack of) alignment of directions of maximum demand at different oscillator periods, and a model to describe the variation of demands at all possible orientations, as well as how they relate to each other, have been described in detail. Being a powerful tool to characterise spectral demands at all possible angles of incidence, its applicability for the design and assessment of structures is apparent, and it offers a means to aid in the further development of strategies to deal with the effects of directionality over different kinds of structures.

The Python code and tools used to generate the MDCS shown herein and in Nievas and Sullivan (2017) can be downloaded from https://github.com/CINievas/MDCS.

8. ACKNOWLEDGMENTS

The authors would like to thank Dr. GraemeWeatherill for fruitful discussions and to acknowledge the Istituto Universitario di Studi Superiori di Pavia, IUSS, for the scholarship to conduct the doctoral research of the first author.

9. REFERENCES

Akkar S, Sandkkaya MA, Senyurt M, Azari Sisi A, Ay BÖ, Traversa P, Douglas J, Cotton F, Luzi L, Hernandez B, Godey S (2014). Reference database for seismic ground-motion in Europe (RESORCE). *Bulletin of Earthquake Engineering*, 12: 311–339.

Baker JW (2011). Conditional mean spectrum: tool for ground-motion selection. *Journal of Structural Engineering*, 137: 322–331.

Boore DM (2010). Orientation-independent, nongeometric-mean measures of seismic intensity from two horizontal components of motion. *Bulletin of the Seismological Society of America*, 100: 1830–1835.

Boore DM, Watson-Lamprey J, Abrahamson N (2006). Orientation-independent measures of ground motion. *Bulletin of the Seismological Society of America*, 96: 1502–1511.

Bozorgnia Y, Abrahamson NA, Al Atik L, Ancheta TD, Atkinson GM, Baker JW, Baltay A, Boore DM, Campbell KW, Chiou BSJ, Darragh R, Day S, Donahue J, Graves RW, Gregor N, Hanks T, Idriss IM, Kamai R, Kishida T, Kottke A, Mahin SA, Rezaeian S, Rowshandel B, Seyhan E, Shahi S, Shantz T, Silva W, Spudich P, Stewart JP, Watson-Lamprey J, Wooddell K, Youngs R (2014). NGA-West2 research project. *Earthquake Spectra*, 30: 973–987.

Der Kiureghian A (1981). A response spectrum method for random vibration analysis of MDF systems. *Earthquake Engineering & Structural Dynamics*, 9: 419–435.

Grant DN (2011). Response spectral matching of two horizontal ground-motion components. *Journal of Structural Engineering*, 137: 289–297.

Hong HP, Goda K (2007). Orientation-dependent ground-motion measure for seismic hazard assessment. *Bulletin of the Seismological Society of America*, 97: 1525–1538.

Jayaram N, Baker JW (2008). Statistical tests of the joint distribution of spectral acceleration values. *Bulletin of the Seismological Society of America*, 98: 2231–2243.

Jayaram N, Lin T, Baker JW (2011). A computationally efficient ground-motion selection algorithm for matching a target response spectrum mean and variance. *Earthquake Spectra*, 27: 797–815.

Kalkan E, Reyes JC (2015). Significance of rotating ground motions on behavior of symmetric- and asymmetric-plan structures: Part II. multi-story structures. *Earthquake Spectra*, 31(3): 1613–1628.

Lagaros ND (2010). The impact of the earthquake incident angle on the seismic loss estimation. *Engineering Structures*, 32: 1577–1589.

Magliulo G, Maddaloni G, Petrone C (2014). Influence of earthquake direction on the seismic response of irregular plan RC frame buildings *Earthquake Engineering & Engineering Vibration*, 13(2): 243–256.

Menun C, Der Kiureghian A (1998). A replacement for the 30%, 40%, and SRSS rules for multicomponent seismic analysis. *Earthquake Spectra*, 14: 153–163.

Nievas CI (2016). Design of structures subject to multidirectional seismic excitation. *PhD thesis*, UME School, IUSS Pavia, Italy.

Nievas CI, Sullivan TJ (2016). Accounting for directionality as a function of structural typology in performance-based earthquake engineering design. *Earthquake Engineering & Structural Dynamics*, 46: 791–809.

Nievas CI, Sullivan TJ (2017). A multidirectional conditional spectrum. *Earthquake Engineering & Structural Dynamics*, in press (Early-View version available online). DOI: 10.1002/eqe.3000

Nievas CI, Sullivan TJ (2018). The variation of ground motions in time. *Under preparation*.

Pagani M, Monelli D, Weatherill G, Danciu L, Crowley H, Silva V, Henshaw P, Butler L, Nastasi M, Panzeri L, Simionato M, Vigano D (2014). OpenQuake engine: an open hazard (and risk) software for the Global Earthquake Model. *Seismological Research Letters*, 85: 692–702.

Rosenblueth E, Contreras H (1977). Approximate design for multicomponent earthquakes. *Journal of the Engineering Mechanics Division*, 103: 881–893.

Shahi SK, Baker JW (2014). NGA-West2 models for ground motion directionality. *Earthquake Spectra*, 30(3): 1285–1300.

Smeby W, Der Kiureghian A (1985). Modal combination rules for multicomponent earthquake excitation. *Earthquake Engineering & Structural Dynamics*, 13: 1–12.

Stewart JP, Abrahamson NA, Atkinson GM, Baker JW, Boore DM, Bozorgnia Y, Campbell KW, Comartin CD, Idriss IM, Lew M, Mehrain M, Moehle JP, Naeim F, Sabol TA (2011). Representation of bidirectional ground motions for design spectra in building codes. *Earthquake Spectra*, 27: 927–937.

Wilson EL, Der Kiureghian A, Bayo EP (1981). A replacement for the SRSS method in seismic analysis. *Earthquake Engineering & Structural Dynamics*, 9: 187–192.